Hindawi Publishing Corporation
Journal of Nanomaterials
Volume 2012, Article ID 328520, 9 pages
doi:10.1155/2012/328520

Research Article

Effect of Surface-Modified Paclitaxel Nanowires on U937 Cells In Vitro: A Novel Drug Delivery Vehicle

Mohamed H. Abumaree,[1] Salem Al-Suwaidan,[2] and Rabih O. Al-Kaysi[1]

[1] *College of Basic Sciences, King Saud bin Abdulaziz University for Health Sciences, National Guard Health Affairs, Riyadh 11426, Saudi Arabia*
[2] *King Abdullah International Medical Research Center, King Abdullah Medical City, National Guard Health Affairs, Riyadh 11426, Saudi Arabia*

Correspondence should be addressed to Rabih O. Al-Kaysi, rabihalkaysi@gmail.com

Received 15 April 2012; Accepted 5 June 2012

Academic Editor: Do Kim

We have fabricated surface-modified paclitaxel nanowires (SM-PNs) with a precise diameter and an average length of 50 μm. The surface of these nanowires is coated with a monolayer of octadecylsiloxane (ODS), which prevents aggregation and enhances dispersivity in aqueous media. This system constitutes a novel drug delivery vehicle based on one-dimensional (1D) nanostructures with a large drug to vehicle ratio. We assayed the cytotoxicity of different diameter SM-PNs (200, 80, 35, and 18 nm) with U937 cells and compared their activity to microcrystalline paclitaxel. SM-PNs reduced U937 cell proliferation in culture followed by cell death. For the same amount of paclitaxel, different diameter SM-PNs displayed different cytotoxic effect at the same incubation time period. SM-PNs with 35 nm diameters were the most efficient in completely halting cell proliferation following the first 24 hours of treatment, associated with 42% cell death. SM-PNs with 18 nm diameters were least effective. These SM-PNs can be tailored to fit a certain treatment protocol by simply choosing the appropriate diameter.

1. Introduction

Many promising anticancer drugs have very low solubility in aqueous and biological media [1, 2]. Low water solubility translates to low bioavailability, which is the "end game" for any novel drug under development [3]. Progress in the field of nanoscience coupled with developing new materials for drug delivery "vehicles" has revived great interest in these drugs by providing a pathway to increase their bioavailability, [4–9] thus making them commercially viable. The widely used anticancer drug paclitaxel [10, 11] (commonly know as Taxol, a registered trademark of Bristol-Myers Squibb) has very low initial water solubility (0.3 μg/mL) [12] despite the presence of several polar functional groups including three hydroxyls. However, this compound is very soluble in organic solvents such as tetrahydrofuran (THF) and dimethyl Sulfoxide (DMSO) making it amenable for nanowire fabrication by solvent annealing inside anodic aluminum oxide (AAO) templates [13]. In order to increase water solubility and bioavailability of paclitaxel, a solubilizing agent is required [12] to encapsulate the drug and disperse it in biological media [14]. Many successful drug delivery vehicle formulations were developed that can incorporate paclitaxel in them prior to in vivo injection. The most commonly used drug delivery vehicle formulation contains chremophor EL, a standard nonionic emulsifier in Paclitaxel chemotherapy [15]. Unfortunately, this vehicle formulation causes anaphylactic shock in some patients [16]. Thus alternative biologically inert vehicle formulations are actively being developed [17–19].

A general way of preparing drug filled nanoparticles is to inject an ethanol or chloroform solution of the drug and emulsifier (usually a nonionic polymer surfactant such as polyethylene glycol PEG, or Chremophor EL) in an aqueous saline or buffered media [20]. This spontaneous self-assembly (a bottom-up approach) yields nanoparticles with variable drug loading [21]. The drug is randomly distributed throughout the vehicle matrix [22] (see Figure 1(a)), along with traces of the organic solvent that fails to evaporate. This nonuniform drug distribution contributes to the burst effect

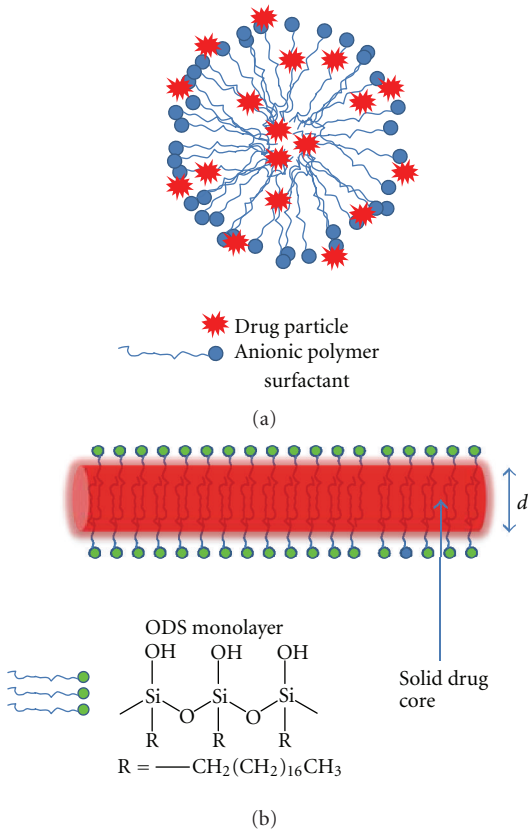

FIGURE 1: (a) Drug-loaded nanoparticle with cluster of drug molecules randomly distributed though out the vehicle matrix. Most of the drug is distributed on the surface of the matrix, which leads to the burst effect. (b) SM-PN with an exact diameter and length. The entire drug is located inside the vehicle (ODS shell). The alkyl group R is anchored inside the drug nanowire with the Si–OH sticking out. ODS stands for octadecylsiloxane.

when the nanoparticles are dispersed in biological media [23]. Preparation of these nanoparticles is usually followed by rigorous analysis to determine the drug loading capacity inside the vehicle matrix as well as their size distribution, which in most cases is broad [24]. Unfortunately, this broad size distribution requires the exclusion of sizes above a certain threshold when administering the drug nanoparticles intravenously, contributing to waste of valuable drug.

In a previous paper we fabricated surface-modified paclitaxel nanowires (SM-PNs) using anodic aluminum oxide (AAO) templates coated with a monolayer of n-octadecylsilane [25]. The diameter and length of the nanowire depend on the pore diameter and thickness of the AAO template, respectively. After releasing the nanowire by dissolving the alumina template in 20% phosphoric acid/0.4% SDS solution, the surface of the nanowires was coated with a monolayer of n-octadecylsiloxane (see Figure 1(b)) that prevented paclitaxel agglomeration and precipitation. In this study, we assayed the cytotoxicity of SM-PNs with diameters 200, 80, 35, and 18 nm and 50 μm long on U937 cells. The effect of SM-PNs on cell proliferation and viability was determined by Trypan blue staining. This study is a proof-of-concept that SM-PNs can function as a drug delivery system for water insoluble drugs, while incorporating a nontoxic octadecylsiloxane (ODS) surface coating as the vehicle.

2. Experimental

2.1. Materials. AAO templates were purchased from two separate sources. Templates with a nominal pore diameter of 200 nm (Anodisc-13) were purchased from Whatman Inc., while precision AAO templates with a narrow pore size distribution (80, 35 and 18 nm) were acquired from Synkera Technologies. All the templates had the same diameter of 1.3 cm and approximate template thickness of 50 μm. n-octadecyltrichlorosilane (95%) was purchased from Acros Organics. Paclitaxel (99%) was acquired from the Selleck Chemical Company and used without further purification. All organic solvents were distilled and stored over activated molecular sieves (3 Å). SEM measurements were performed using JEOL JSM-6510LV scanning electron microscope. Samples were sputter coated with Pt prior to scanning. Gravimetric analysis was performed using Sartorius SE2 Ultra Micro Balance with 0.1 μg precision. UV-Vis measurements were done using Spectro UV-Vis Double beam (UVD-2950) spectrophotometer from Labomed. The human monocytic cell line (U937) was obtained from Health Protection Agency (HPA), UK. Trypan blue was purchased from Invitrogen, Saudi Arabia. Different diameter SM-PNs suspensions in 20% phosphoric acid/0.4% SDS were stored at −150°C until further use.

(a) Preparation of SM-PNs: these nanowires were prepared as described previously [25]. The concentration of paclitaxel in the form of SM-PNs was adjusted to 580 μg/mL by adding the appropriate amount of 20% phosphoric acid/0.4% SDS.

(b) Preparation of microcrystalline paclitaxel or free paclitaxel (FT): a solution of paclitaxel in THF (1.8 mg in 100 μL) was rapidly injected into 3 mL of stirred solution containing 20% phosphoric acid/0.4% SDS. The mixture becomes turbid with the formation of a suspension of paclitaxel microcrystals (580 μg/mL).

(c) Scanning Electron Microscopy (SEM): a drop of the paclitaxel microcrystalline suspension was filtered through a 20 nm pore diameter AAO template then washed with 0.2 mL deionized (D.I.) water before air-drying at room temperature. The AAO template/paclitaxel microcrystal residue was fixed on an SEM stub via conducting carbon tape and sputter coated with Pt (~5 nm thickness).

(d) Fabrication of multilayered ODS shells: an AAO template (Synkera, 80, 35, 18 m) or Whatman (200 nm pore diameter) was sonicated with ethanol then hexane prior to drying in an oven set at 120°C for 2 hours. The template was placed over a fritted funnel and suction applied. A 5% solution of n-octadecyltrichlorosilane (OTS) in hexane was filtered

through 0.1 mL at a time followed by 0.1 mL of water-saturated benzene to hydrolyze the Si–Cl bond and form a reactive Si–OH handle. The process was repeated several times till the AAO pores become clogged and the hexane solution wont filter through. The template was air dried, polished with 1500 grit abrasive paper then dried in an oven at 120°C for 2 hours. The multilayered ODS shells were liberated by dissolving the template in 20% H_3PO_4/0.4% SDS.

(e) In Vitro assay: human monocytic U937 cancer cells (1.8×10^6/well) were cultured in a 6-well culture plate with 3 mL of RPMI-1640 medium containing 10% fetal bovine serum (FBS), 100 mg/mL of L-glutamate, 100 mg/mL streptomycin, 100 U/L penicillin, and 3 μg of Paclitaxel in SM-PNs (200 nm, 80 nm, 35 nm and 18 nm) or FT suspension in 20% H_3PO_4/0.4% SDS. The cells were then incubated at 37°C for a period of 24 h, 48 h, and 72 h in a humidified atmosphere containing 5% CO_2 and 95% air. For comparison, untreated U937 cells served as a negative control. Each experiment was performed in duplicates. Following washing cells with phosphate buffered saline (PBS, pH 7.4) for two times, a sample cell suspension was mixed with an equal volume of 0.4% Trypan blue to stain nonviable cells [26]. A 10 μL sample was added to the hemocytometer chamber. Cells were then allowed to settle down for 3 minutes before viable and dead cells were then counted using a light microscope. Cells from each SM-PN size were counted three times and the results combined with the duplicate experiment, to give us a total of 6 counts for each SM-PN diameter.

(f) UV-Vis measurement of paclitaxel concentration in PBS solution: A templated sample of paclitaxel in AAO was submerged in a vial containing 25 mL of PBS. The vial was placed in a water bath set at 37°C and slowly agitated for two days. A sample of the buffer solution was measured using UV-Vis every 12 hour. To determine the paclitaxel concentrations from the absorption spectrum, absorption coefficient at the peak of the absorption was taken to be (ε/dm^{-3} mol^{-1} cm^{-1} 29 800) [27] at λ_{max} (MeOH)/nm = 227. At the end of the experiment the template was removed, rinsed with distilled water, and dried under vacuum before being weighed using a microbalance. The mass difference was close to 2 μg reflecting the amount of paclitaxel dissolved out from the template into 25 mL of PBS solution.

3. Results and Discussions

There are several benefits from using nanowires or 1D nanostructures as drug carriers over nanoparticles or 0-dimensional (0D) nanostructures. Nanowires tend to incorporate inside cells more efficiently than nanoparticles [28, 29]. The latter has to deform and squeeze in order to penetrate the cell wall [30]. On the other hand, the large aspect ratio and slender features of the nanowire allows it to swim better and circulate for longer periods in biological media without exclusion from the system [31, 32]. This gave us impetus to design 1D drug nanostructures with large aspect ratios. To the best of our knowledge, there are no reports on the cytotoxic effect of 1D nanostructures (nanowires or nanorods) composed of a solid drug core. Most of the 1D nanostructures used in nanomedicine are based on inorganic or polymer core carriers with drug covalently bonded or adsorbed in the matrix of the vehicle [33–35].

As mentioned earlier, the high solubility of paclitaxel in organic solvents makes it amenable to nanowire formation via solvent annealing inside AAO templates with any pore sizes or template thickness. In a previous paper, we employed a stepwise bottom-up approach to fabricate surface-modified paclitaxel nanowires (SM-PNs) using AAO templates with precise pore diameter and template thickness [25]. The size, ratio of surface coating to drug, and shape of the SM-PN were determined accurately using gravimetric methods and electron microscopy (see Figure 2). The hydrophilic monolayer of ODS is tethered to the paclitaxel nanowire surface through the n-octadecyl end (see Figure 1(b)). In turn, siloxy end of the ODS layer behaves as a pseudo vehicle which prevents the nanowires from agglomerating and protects the drug from degradation and hydrolysis [25]. These SM-PNs were liberated from the AAO template using 20% H_3PO_4 in 0.4% SDS. The nanowires are well dispersed in aqueous media such that for the same concentration of paclitaxel, SM-PNs with diameter less than 80 nm appear clear because they do not scatter visible light, while microcrystalline paclitaxel scatters light giving a turbid suspension as seen in Figure 3.

The tethered surface coating of ODS in SM-PNs presents a unique vehicle where the coating does not have to be above a certain critical micelle concentration (CMC) to surround the drug and thus can be diluted without the risk of dissociating from the surface. The ratio of ODS to drug was determined gravimetrically for each SM-PN diameter. The benefits from the stepwise bottom-up templated approach are a typical paclitaxel loading of 75% for a 35 nm diameter SM-PNs. This is not the case with micelleular-, liposome- or polymer-based drug nanoparticles where encapsulation efficiency and drug loading capacity are usually small and variable [36] which can load the biological system with unnecessary vehicle matrix. A major advantage in using SM-PNs is the absence of paclitaxel on the surface of the nanowire Figure 1(b). The stepwise bottom-up fabrication procedure solvent anneals paclitaxel inside the ODS shell which in turn is covalently bonded to the pore surface of the AAO template. After solvent annealing, the drug-laden template can be placed under high vacuum to remove the last traces of the annealing solvent used before dissolving the template.

3.1. In Vitro Assay. In order to test whether SM-PNs retain their cytotoxic potential, we studied the effects of these nanowires on U937 cells. To rule out the cytotoxicity of the ODS layer, empty ODS shells of different diameters (200, 80, 35, and 18 nm) were incubated with U937 cells culture for a period of two days. ODS shells had no effect. However, testing empty ODS shells was problematic

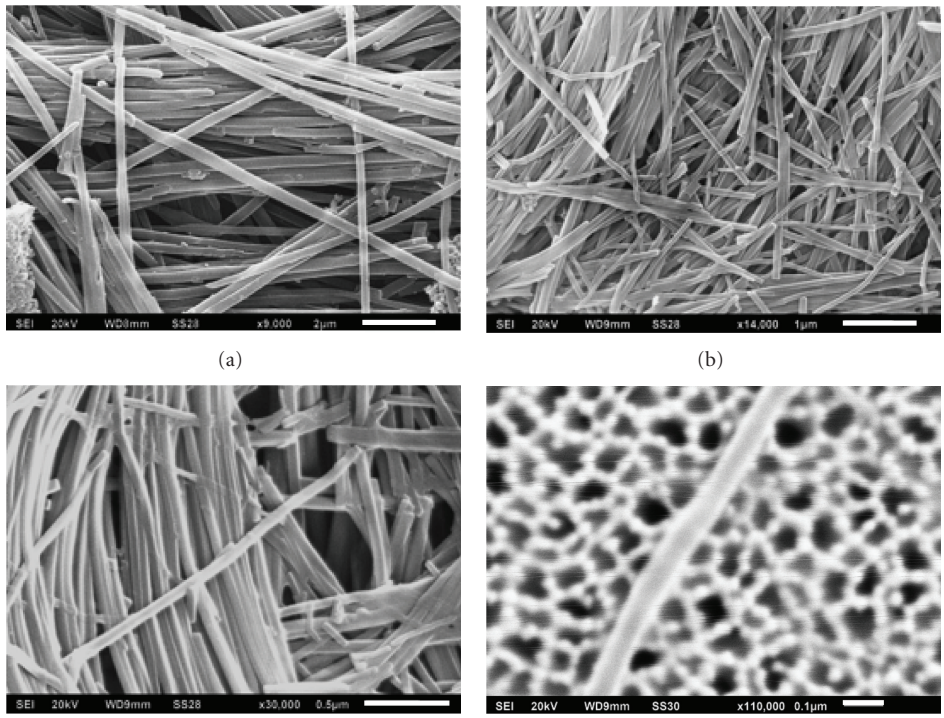

(a) (b) (c) (d)

Figure 2: (a) SEM image of SM-PNs with 200 nm diameters. (b) SEM image of 80 nm SM-PNs bundles. (c) SEM image of 35 nm SM-PNs over AAO template. (d) Close-up image of a single 35 nm SM-PN over an AAO template. The AAO pores in the background have an average diameter of 40 nm.

(a) (b) (c)

Figure 3: Vials containing paclitaxel in 20% H_3PO_4/0.4% SDS. (a) 580 μg of paclitaxel microcrystals (FT). (b) 580 μg of paclitaxel in the form of SM-PNs with 200 nm diameter and 50 μm long. (c) 580 μg of paclitaxel in the form of SM-PNs with 35 nm diameter and 50 μm long. For comparison, note the visibility of the bottom rim of the vial. Each vial contains around 1 mL of 20% H_3PO_4/0.4% SDS.

because these monolayers are too thin and will collapse once they are released from the template because of their hydrophobic core. Collapsed ODS shells might not reflect a clear evaluation of the ODS cytotoxicity in a nanowire form. Therefore the shells were stiffened by casting several layers of OTS (n-Octadecyltrichlorosilane) inside the shell via multiple dip drying cycles [37] forming a spongy matrix of cross-linked OTS monomers. Experiments revealed that neither the shape (diameter and length) of the nanowire nor the ODS material has any cytotoxic effect on the U937 cells and did not affect the proliferation rate of the cells. The ratio of multicoated ODS shell to U937 cells was as shown in Table 1. This puts the ratio bellow any cytotoxic limit that may induce necrotic death in cells [38–40].

Table 1: Number of SM-PNs containing 3 μg paclitaxel.

SM-PN diameter (nm)	*Total number of SM-PNs ($\times 10^6$)	Ratio of SM-PN to U937 cells
200	2.8	2 : 1
80	19	10 : 1
35	66	37 : 1
18	499	277 : 1

* The average SM-PN length is ~50 μm ± 5 μm.

The next step was to study the cytotoxicity of different diameter SM-PNs and compare their cytotoxicity to that of free paclitaxel (FT). A bulk suspension of SM-PNs in 20% phosphoric acid and 0.4% SDS was used. On average it requires 5 μL of this suspension to be added to the cell culture, in order to provide 3 μg of paclitaxel. The effect of the tiny amount of Phosphoric acid and SDS on U937

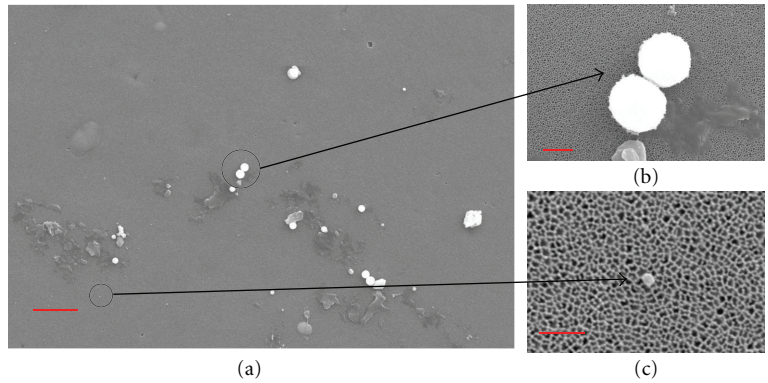

Figure 4: Scanning electron micrograph of microcrystalline paclitaxel or free paclitaxel (FT) over an AAO template. (a) Microcrystalline paclitaxel aggregate over an AAO template. Scale bare = 10 μm. (b) A pair of paclitaxel microspheres. Scale bare = 1 μm. (c) A spherically shaped paclitaxel nanoparticle. Scale bar = 500 nm.

cell proliferation and death was assayed and compared to the untreated U937 culture. Both cell proliferation and cell death were not affected. The added phosphoric acid was neutralized by the culture medium to produce phosphate salts with minimum impact on the cell culture medium pH. Microcrystalline paclitaxel or free paclitaxel (FT) was prepared by rapidly injecting a tetrahydrofuran (THF) solution of paclitaxel in 20% phosphoric acid/0.4% SDS mixture. A visible suspension of microcrystalline paclitaxel slowly materializes over the course of several minutes. An SEM image of the free paclitaxel microcrystals reveals a broad size distribution with mostly spherical shaped microparticles ranging in size from 2 to 0.1 μm in diameter (see Figure 4).

The SM-PN diameters investigated in this study were 200 nm, 80 nm, 35 nm, and 18 nm. A total of 1.8×10^6 U937 cells were incubated with 3 μg of paclitaxel in the form of SM-PNs. The solubility of paclitaxel in pure water is around 0.3 μg/mL [41], and is significantly reduced to less than 0.1 μg/mL in PBS solution [42]. To confirm this result, templated SM-PNs (200, 35, and 18 nm) were suspended in 25 mL of PBS over a period of 2 days at 37°C. The amount of paclitaxel released from the template was measured using UV-Vis. In the first 24 hours the amount of paclitaxel released was below the detection limit of the UV-Vis ($OD_{227\,nm} < 0.001$). After 48 hours the amount of paclitaxel released was around 0.1 μg/mL of PBS solution, calculated from the OD of the solution at 227 nm. In order to get a better estimate of the amount of paclitaxel released, we utilized an ultramicrobalance to gravimetrically determine the amount of paclitaxel dissolved out of the template. The amount of paclitaxel released from the template was ~2 μg in 25 mL of PBS solution (0.08 μg paclitaxel in 1 mL of buffer). In a different setup we suspended SM-PNs (200 nm diameter) in 25 mL of PBS solution at 37°C for 48 hours. The mixture was centrifuged to separate the suspended nanowires and the absorption spectrum of the PBS solution collected. The amount of paclitaxel dissolved was calculated to be around 0.11 μg/mL of buffer. Thus it is safe to assume that the paclitaxel inside the ODS shell will have a negligible solubility in the culture media. The ratio of SM-PNs to U937 cells depends on the diameter of the nanowire. Assuming that all nanowires have approximately the same length of 50 μm we calculate the total number of SM-PNs needed to yield 3 μg of paclitaxel in every 3 mL culture of U937 cells (Table 1).

As shown in Table 1, the highest ratio of SM-PNs to U937 cells is still below the cytotoxic limit that may cause cell necrosis [38–40]. This was also confirmed earlier when we studied the cytotoxicity of multilayered ODS shells. In addition, a large number of cells were used in this study in order to dilute out effects due to the tiny amount of soluble paclitaxel.

In chemotherapy one of the primary goals is to slow down or stop cancer cell proliferation during the early stages of administering the drug. paclitaxel stabilizes tubule polymerization and stops cell division; thus it acts on inhibiting cell proliferation and then inducing apoptosis in cells [43–46]. In this study, we examined the ability of SM-PNs to inhibit U937 cell proliferation. Trypan Blue exclusion test was used to determine cell viability following treatment with SM-PNs. During culture, the cell proliferation rate of untreated U937 cells is almost double every 24 hours, but in the FT sample; cell proliferation was increased by 39% after the first 24 hours. Interestingly, U937 cells treated with SM-PNs had a lower proliferation capacity. The most effective size in inhibiting cell proliferation was the 35 nm (0%) after 24 hours in culture. In addition, this nanowire size caused rapid cell death (42%) after 24 hours in culture. Upon exposure to paclitaxel, U937 cells swell up with the appearance of vacuoles Figure 5. This is a typical morphology for cells exposed to paclitaxel [47–49]. During the first 24 hours of incubation, all the paclitaxel samples caused an average of 42% cell death. After 72 hours in culture, SM-PNs of all sizes caused 100% cell death while the FT lingered behind with only 89% cell death (Figure 6). As shown in Table 2, there is loss in the total number of cells after treatment as a result of cell membrane rupture, a sign of necrotic death [50]. Our results demonstrate that SM-PNs can induce apoptosis and necrosis in U937 cells as it has been previously reported for free paclitaxel [51], thus suggesting that using SM-PNs as a vehicle to deliver paclitaxel into cells is not affecting the death mechanism of the drug. However,

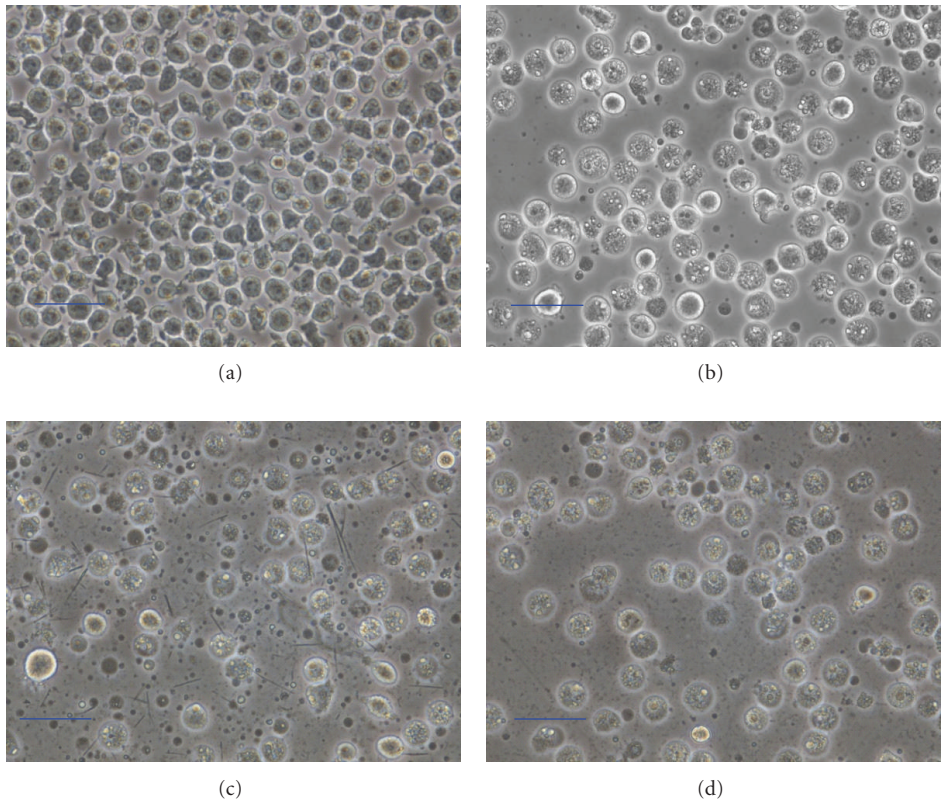

Figure 5: Optical microscope images of U937 cells. (a) Untreated U937 cells. The cells tend to be asymmetrical with a dark center. (b) U937 cells treated with FT after 72 hours. Notice the pronounced swelling and appearance of vacuoles (white dots in the middle). (c) U937 cells treated with 200 nm diameter SM-PNs after 72 hours of incubation. Nanowires are visible in the background with the presence of cellular debris. (d) U937 cells treated with 35 nm diameter SM-PNs after 72 hours of incubation. The nanowires are too small to be viewed at this magnification. Cellular debris from burst cells appear as specs in the background. Scale bar = 10 μm.

more work is needed to elucidate the death mechanisms of SM-PNs.

The solubility experiment has provided some mechanistic evidence that there is no significant dissolution of paclitaxel out of the ODS shell that may inhibit cell proliferation. Therefore, it is possible that SM-PNs should physically contact with the cells in order to affect them. To eliminate the possibility that the tiny amount of dissolved paclitaxel is causing a significant impact on the cell proliferation, we incubated the same number of U937 cells (1.8×10^6) with SM-PNs embedded inside a 200 nm AAO template. A small peace of the paclitaxel-loaded AAO template (90 μg) containing an equivalent to 3 μg of embedded paclitaxel was secured to one side of the culture well to avoid direct contact with the cells. The culture plate was gently swirled every 6 hours for even distribution of dissolved paclitaxel. After 24 hours the cell proliferation rate was only slightly affected with -3% difference when compared to the untreated sample and a 6% cell death compared to the natural cell death of 4.5% of the untreated U937 sample. The 48 h and 72 h had only subtle differences when compared with the untreated U937 sample. Judging from cell proliferation, it seems that the effect of SM-PNs increases as the diameter of the nanowires becomes smaller. The 18 nm SM-PNs present an unexpected result. After the first 24 hours, the 18 nm SM-PNs increased cell proliferation (58%). This was associated with 43% cell death. This may suggest an optimum size for cellular uptake of the nanowires. For nanoparticles, the optimum size is around 50 nm [52]. If we factor in the hydrodynamic radius of the 35 nm diameter SM-PN we would most likely approach a size close to 50 nm. This result may provide us with added insight into the mechanism through which the drug is being introduced into the cells. It seems that the nanowires not only have to be close or on the cell but they somehow have to penetrate the cell membrane via endocytosis. For SM-PNs with an 18 nm diameter, paclitaxel constitutes around 30% of the mass of the nanowire with the rest being ODS shell (70%). Most of the paclitaxel is adsorbed on the surface of the n-octadecyl layer. This adsorption can slow down the release of paclitaxel inside the cell due to partition. Nonetheless the percentage of dead cells in the first 24 hours was 43%, which suggests that the drug is being liberated inside the cells at a slower rate.

4. Conclusion

SM-PNs of different diameters were fabricated and their cytotoxicity on U937 cells was studied in vitro. For the same ratio of paclitaxel/cells, the most efficient SM-PNs had a diameter of 35 nm with a complete inhibition of cell

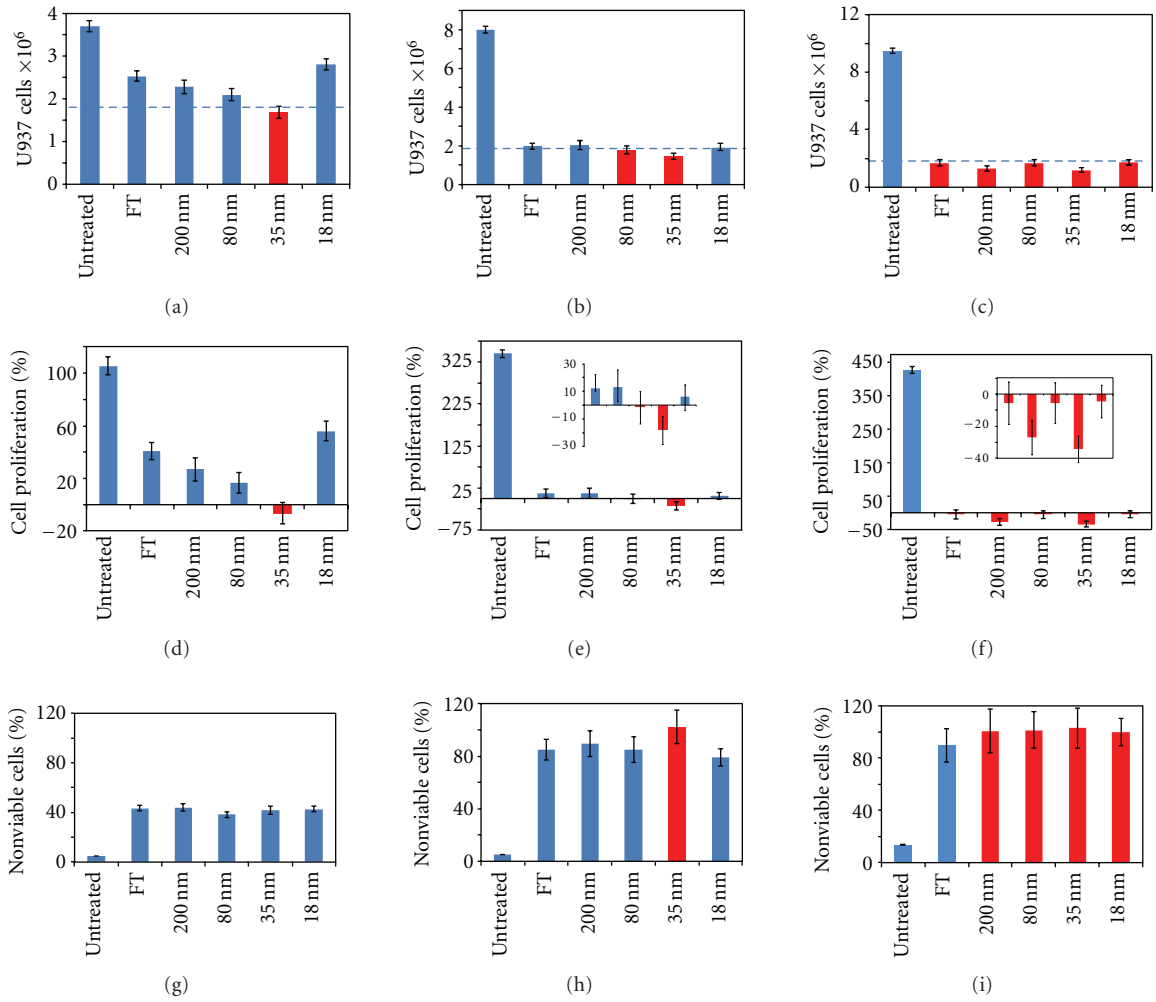

Figure 6: (a, b, c) Total number of U937 cells with different paclitaxel forms after 24, 48, and 72 h, respectively. Dotted line represents the initial number of cells (1.8×10^6). (d, e, f) % cell proliferation with different paclitaxel forms after 24, 48, and 72 h, respectively. Incept: expanded view of the paclitaxel region. (g, h, i) % nonviable cells at 24, 48, and 72 h, respectively.

Table 2: 24, 48, and 72 hour incubation periods, respectively.

Time	Parameter	Untreated	FT	SM-PN 200 nm	SM-PN 80 nm	SM-PN 35 nm	SM-PN 18 nm
24 h	Total cells* (SD)	3.70 (0.126)	2.53 (0.12)	2.28 (0.16)	2.10 (0.14)	1.68 (0.15)	2.81 (0.13)
	Nonviable cells* (SD)	0.18 (0.006)	1.12 (0.05)	1.02 (0.07)	0.81 (0.05)	0.71 (0.06)	1.22 (0.057)
	% Nonviable (SD)	4.9 (0.17)	43.5 (2.07)	44.0 (3.1)	38.2 (2.6)	41.8 (3.6)	42.8 (2.12)
	% Proliferation (SD)	106 (7.03)	40.7 (6.73)	26.8 (8.90)	16.7 (7.85)	−6.5 (8.17)	56 (7.53)
48 h	Total cells (SD)	7.98 (0.16)	2.02 (0.18)	2.03 (0.22)	1.78 (0.19)	1.48 (0.17)	1.91 (0.15)
	Nonviable cells (SD)	0.40 (0.008)	1.69 (0.15)	1.82 (0.20)	1.50 (0.13)	1.47 (0.17)	1.49 (0.12)
	% Nonviable (SD)	5.0 (0.10)	84.9 (7.93)	89.4 (9.7)	85.0 (9.8)	100 (12.8)	79.0 (6.6)
	% Proliferation (SD)	344 (8.90)	12.0 (10.2)	13.0 (12.5)	−0.9 (10.8)	−17.6 (9.5)	6.0 (8.7)
72 h	Total cells (SD)	9.48 (0.18)	1.70 (0.24)	1.32 (0.19)	1.70 (0.23)	1.18 (0.15)	1.72 (0.18)
	Nonviable cells (SD)	1.30 (0.025)	1.50 (0.21)	1.31 (0.19)	1.69 (0.23)	1.18 (0.15)	1.70 (0.18)
	% Nonviable (SD)	13.7 (0.26)	89.7 (12.6)	100 (16.5)	100 (13.8)	100 (15.3)	99.9 (10.4)
	% Proliferation (SD)	427 (10.2)	−5.5 (13.1)	−26.8 (10.7)	−5.65 (12.7)	−34.2 (8.2)	−4.6 (10.2)

SD: standard deviation.
*Total number of nonviable or viable cells ($\times 10^6$).
% nonviable cells = (number of nonviable cells)/Total number of cells × 100.
% Proliferation = (Total number of cells − initial number of cells)/initial number of cells × 100.

proliferation in the first 24 hours of incubation. Different size nanowires have shown different effects on cell proliferation rate. This difference rules out the possibility that paclitaxel dissolved out of the ODS shell prior to interaction with the cell. It is still an open question concerning the mechanism of action. In this proof-of-concept, we have shown that by utilizing a simple solvent annealing method inside surface-modified AAO templates, we can generate SM-PNs with tailored cytotoxicity using a novel drug delivery vehicle.

Acknowledgments

R. O. Al-Kaysi acknowledges the support of KSAU-HS/KAIMRC through Grants RC08/093 and RC10/104 and King Abdulaziz City for Science and Technology (KACST) through Grant AT-30-435. The authors greatly acknowledge Professor C. J. Bardeen of the Department of chemistry, University of California Riverside for helpful discussions.

References

[1] F. Danhier, N. Lecouturier, B. Vroman et al., "Paclitaxel-loaded PEGylated PLGA-based nanoparticles: in vitro and in vivo evaluation," *Journal of Controlled Release*, vol. 133, no. 1, pp. 11–17, 2009.

[2] J. H. M. Schellens, M. M. Malingré, C. M. Kruijtzer et al., "Modulation of oral bioavailability of anticancer drugs: from mouse to man," *European Journal of Pharmaceutical Sciences*, vol. 12, no. 2, pp. 103–110, 2000.

[3] V. B. Patravale, A. A. Date, and R. M. Kulkarni, "Nanosuspensions: a promising drug delivery strategy," *Journal of Pharmacy and Pharmacology*, vol. 56, no. 7, pp. 827–840, 2004.

[4] Y. N. Usha, T. T. Angel, and N. Udupa, "Nanotechnology: perspectives on solubility/bioavailability enhancement Pharma," *Review*, vol. 8, no. 45, pp. 59–66, 2010.

[5] C. Kaparissides, S. Alexandridou, K. Kotti, and S. Chaitidou, "Recent advances in novel drug delivery systems," *Journal of Nanotechnology Online*, vol. 2, pp. 1–11, 2006.

[6] P. D. Reddy and D. Swarnalatha, "Recent advances in novel drug delivery systems," *International Journal of PharmTech Research*, vol. 2, no. 3, pp. 2025–2027, 2010.

[7] G. A. Hughes, "Nanostructure-mediated drug delivery," *Nanomedicine*, vol. 1, no. 1, pp. 22–30, 2005.

[8] M. M. De Villiers, P. Aramwit, and G. S. Kwon, *Nanotechnology in Drug Delivery*, vol. 10, Springer, 2009.

[9] K. K. Jain, "Nanotechnology-based drug delivery for cancer," *Technology in Cancer Research and Treatment*, vol. 4, no. 4, pp. 407–416, 2005.

[10] C. M. Spencer and D. Faulds, "Paclitaxel: a review of its pharmacodynamic and pharmacokinetic properties and therapeutic potential in the treatment of cancer," *Drugs*, vol. 48, no. 5, pp. 794–847, 1994.

[11] M. A. Jordan and L. Wilson, "Microtubules as a target for anticancer drugs," *Nature Reviews Cancer*, vol. 4, no. 4, pp. 253–265, 2004.

[12] S. C. Lee, K. M. Huh, J. Lee, Y. W. Cho, R. E. Galinsky, and K. Park, "Hydrotropic polymeric micelles for enhanced paclitaxel solubility: in vitro and in vivo characterization," *Biomacromolecules*, vol. 8, no. 1, pp. 202–208, 2007.

[13] R. O. Al-Kaysi and C. J. Bardeen, "General method for the synthesis of crystalline organic nanorods using porous alumina templates," *Chemical Communications*, no. 11, pp. 1224–1226, 2006.

[14] A. K. Singla, A. Garg, and D. Aggarwal, "Paclitaxel and its formulations," *International Journal of Pharmaceutics*, vol. 235, no. 1-2, pp. 179–192, 2002.

[15] A. Sparreboom, L. Van Zuylen, E. Brouwer et al., "Cremophor EL-mediated alteration of paclitaxel distribution in human blood: clinical pharmacokinetic implications," *Cancer Research*, vol. 59, no. 7, pp. 1454–1457, 1999.

[16] H. Gelderblom, J. Verweij, K. Nooter, and A. Sparreboom, "Cremophor EL: the drawbacks and advantages of vehicle selection for drug formulation," *European Journal of Cancer*, vol. 37, no. 13, pp. 1590–1598, 2001.

[17] J. M. Meerum Terwogt, B. Nuijen, W. W. Ten Bokkel Huinink, and J. H. Beijnen, "Alternative formulations of paclitaxel," *Cancer Treatment Reviews*, vol. 23, no. 2, pp. 87–95, 1997.

[18] S. Khandavilli and R. Panchagnula, "Nanoemulsions as versatile formulations for paclitaxel delivery: peroral and dermal delivery studies in rats," *Journal of Investigative Dermatology*, vol. 127, no. 1, pp. 154–162, 2007.

[19] L. He, G. L. Wang, and Q. Zhang, "An alternative paclitaxel microemulsion formulation: hypersensitivity evaluation and pharmacokinetic profile," *International Journal of Pharmaceutics*, vol. 250, no. 1, pp. 45–50, 2003.

[20] C. Pinto Reis, R. J. Neufeld, A. J. Ribeiro, and F. Veiga, "Nanoencapsulation I. Methods for preparation of drug-loaded polymeric nanoparticles," *Nanomedicine*, vol. 2, no. 1, pp. 8–21, 2006.

[21] X. Gu, A novel approach to formulation of anticancer drugs in nanoparticles Ph.D. thesis, 2008.

[22] X. Gu, "Drug-loaded nanoparticles preparation methods and drug targeting issues," *European Journal of Pharmaceutics and Biopharmaceutics*, vol. 39, pp. 173–191, 1993.

[23] X. Huang and C. S. Brazel, "On the importance and mechanisms of burst release in matrix-controlled drug delivery systems," *Journal of Controlled Release*, vol. 73, no. 2-3, pp. 121–136, 2001.

[24] D. Y. Kang, M. J. Kim, S. T. Kim, K. S. Oh, S. H. Yuk, and S. Lee, "Size characterization of drug-loaded polymeric core/shell nanoparticles using asymmetrical flow field-flow fractionation," *Analytical and Bioanalytical Chemistry*, vol. 390, no. 8, pp. 2183–2188, 2008.

[25] M. H. Abumaree, L. Zhu, C. J. Bardeen, S. D. Al-Suwaidan, and R. O. Al-Kaysi, "Fabrication of biologically active surface-modified Taxol nanowires using anodic aluminum oxide templates," *RSC Advances*, vol. 1, no. 5, pp. 884–892, 2011.

[26] W. Strober, "Trypan blue exclusion test of cell viability," in *Current Protocols in Immunology*, John Wiley and Sons, 2001.

[27] *Merck Index*, 12 edition, 1996.

[28] S. E. A. Gratton, P. A. Ropp, P. D. Pohlhaus et al., "The effect of particle design on cellular internalization pathways," *Proceedings of the National Academy of Sciences of the United States of America*, vol. 105, no. 33, pp. 11613–11618, 2008.

[29] S. Venkataraman, J. L. Hedrick, Z. Y. Ong et al., "The effects of polymeric nanostructure shape on drug delivery," *Advanced Drug Delivery Reviews*, vol. 63, no. 14-15, pp. 1228–1246, 2011.

[30] M. E. Fox, F. C. Szoka, and J. M. J. Fréchet, "Soluble polymer carriers for the treatment of cancer: the importance of molecular architecture," *Accounts of Chemical Research*, vol. 42, no. 8, pp. 1141–1151, 2009.

[31] O. S. Pak, W. Gao, J. Wang, and E. Lauga, "High-speed propulsion of flexible nanowire motors: theory and experiments," *Soft Matter*, vol. 7, no. 18, pp. 8169–8181, 2011.

[32] Y. Geng, P. Dalhaimer, S. Cai et al., "Shape effects of filaments versus spherical particles in flow and drug delivery," *Nature Nanotechnology*, vol. 2, no. 4, pp. 249–255, 2007.

[33] J. H. Park, G. von Maltzahn, L. Zhang et al., "Systematic surface engineering of magnetic nanoworms for in vivo tumor targeting," *Small*, vol. 5, no. 6, pp. 694–700, 2009.

[34] S. J. Son, X. Bai, A. Nan, H. Ghandehari, and S. B. Lee, "Template synthesis of multifunctional nanotubes for controlled release," *Journal of Controlled Release*, vol. 114, no. 2, pp. 143–152, 2006.

[35] W. Zhou, P. Gao, L. Shao et al., "Drug-loaded, magnetic, hollow silica nanocomposites for nanomedicine," *Nanomedicine*, vol. 1, no. 3, pp. 233–237, 2005.

[36] L. Mu, M. B. E. Chan-Park, C. Y. Yue, and S. Feng, "Pharmaceutical properties of nanoparticulate formulation composed of TPGS and PLGA for controlled delivery of anticancer drug," http://dspace.mit.edu/handle/1721.1/3916.

[37] A. Sah, H. L. Castricum, A. Bliek, D. H. A. Blank, and J. E. Ten Elshof, "Hydrophobic modification of γ-alumina membranes with organochlorosilanes," *Journal of Membrane Science*, vol. 243, no. 1-2, pp. 125–132, 2004.

[38] A. Adili, S. Crowe, M. F. Beaux et al., "Differential cytotoxicity exhibited by silica nanowires and nanoparticles," *Nanotoxicology*, vol. 2, no. 1, pp. 1–8, 2008.

[39] D. C. Julien, C. C. Richardson, M. F. Beaux, D. N. McIlroy, and R. A. Hill, "In vitro proliferating cell models to study cytotoxicity of silica nanowires," *Nanomedicine*, vol. 6, no. 1, pp. 84–92, 2010.

[40] A. Nan, X. Bai, S. J. Son, S. B. Lee, and H. Ghandehari, "Cellular uptake and cytotoxicity of silica nanotubes," *Nano Letters*, vol. 8, no. 8, pp. 2150–2154, 2008.

[41] F. M. Musteata and J. Pawliszyn, "Determination of free concentration of paclitaxel in liposome formulations," *Journal of Pharmacy and Pharmaceutical Sciences*, vol. 9, no. 2, pp. 231–237, 2006.

[42] D.-H. Kwak, J.-B. Yoo, and D. J. Kim, "Drug Release behavior from nanoporous anodic aluminum oxide," *Journal of Nanoscience and Nanotechnology*, vol. 10, no. 1, pp. 345–348, 2010.

[43] S. J. Park, C. H. Wu, J. D. Gordon, X. Zhong, A. Emami, and A. R. Safa, "Taxol induces caspase-10-dependent apoptosis," *The Journal of Biological Chemistry*, vol. 279, no. 49, pp. 51057–51067, 2004.

[44] C. Von Haefen, T. Wieder, F. Essmann, K. Schulze-Osthoff, B. Dörken, and P. T. Daniel, "Paclitaxel-induced apoptosis in BJAB cells proceeds via a death receptor-independent, caspases-3/-8-driven mitochondrial amplification loop," *Oncogene*, vol. 22, no. 15, pp. 2236–2247, 2003.

[45] A. Vantieghem, Y. Xu, Z. Assefa et al., "Phosphorylation of Bcl-2 in G_2/M phase-arrested cells following photodynamic therapy with hypericin involves a CDK1-mediated signal and delays the onset of apoptosis," *The Journal of Biological Chemistry*, vol. 277, no. 40, pp. 37718–37731, 2002.

[46] X.-P. Wang, T.-S. Chen, L. Sun, J.-Y. Cai, M.-Q. Wu, and M. Mok, "Live morphological analysis of taxol-induced cytoplasmic vacuoliazation in human lung adenocarcinoma cells," *Micron*, vol. 39, no. 8, pp. 1216–1221, 2008.

[47] I. Androic, A. Krämer, R. Yan et al., "Targeting cyclin B1 inhibits proliferation and sensitizes breast cancer cells to taxol," *BMC Cancer*, vol. 8, article 391, 2008.

[48] M. A. Tichomirowa, M. Theodoropoulou, A. F. Daly et al., "Toll-like receptor-4 is expressed in meningiomas and mediates the antiproliferative action of paclitaxel," *International Journal of Cancer*, vol. 123, no. 8, pp. 1956–1963, 2008.

[49] L. Vicari, T. Musumeci, I. Giannone et al., "Paclitaxel loading in PLGA nanospheres affected the in vitro drug cell accumulation and antiproliferative activity," *BMC Cancer*, vol. 8, article 212, 2008.

[50] P. Golstein and G. Kroemer, "Cell death by necrosis: towards a molecular definition," *Trends in Biochemical Sciences*, vol. 32, no. 1, pp. 37–43, 2007.

[51] P. C. Liao and C. H. Lieu, "Cell cycle specific induction of apoptosis and necrosis by paclitaxel in the leukemic U937 cells," *Life Sciences*, vol. 76, no. 14, pp. 1623–1639, 2005.

[52] S. Zhang, J. Li, G. Lykotrafitis, G. Bao, and S. Suresh, "Size-dependent endocytosis of nanoparticles," *Advanced Materials*, vol. 21, no. 4, pp. 419–424, 2009.